The Self-Assembly of a Lipophilic Deoxyguanosine Derivative and the Formation of a Liquid-Crystalline Phase in Hydrocarbon Solvents

by **Giovanni Gottarelli***, **Stefano Masiero**, **Elisabetta Mezzina***, and **Gian Piero Spada**

Università di Bologna, Dipartimento di Chimica Organica A. Mangini, Via S. Donato 15, I-40127 Bologna

and **Paolo Mariani***

Università di Ancona, Istituto di Scienze Fisiche e INFN (Unità di Ancona), Via Ranieri 65, I-60131 Ancona

and **Maurizio Recanatini**

Università di Bologna, Dipartimento di Scienze Farmaceutiche, Via Belmeloro 6, I-40126 Bologna

Dedicated to Professor *Stephen F. Mason*, F.R.S., on the occasion of his 75th birthday

The lipophilic 3′,5′-di-*O*-decanoyl-2′-deoxyguanosine (**1**) in $CHCl_3$ undergoes extensive self-assembly, mediated by H-bonding between the guanine bases, to give ribbon-like aggregates. X-Ray investigation of the platelets obtained from $CHCl_3$ reveals a disordered fibre-like structure consisting of stacks of the ribbon-like aggregates. The aggregates are completely different from the columnar structures, based on G-quartets, which are the building blocks of the mesophases formed by deoxyguanosine oligonucleotides in H_2O. In pure hydrocarbons or in $CHCl_3$/hydrocarbons, **1** forms a lyotropic liquid-crystalline phase.

1. Introduction. – Among nucleobases, guanine possesses a unique sequence of groups which act as donors or acceptors of H-bonds (*Fig. 1*). These groups are of fundamental importance in the self-recognition and self-assembly processes which occur through the formation of *Hoogsteen* H-bonded quartets (G-quartets) in H_2O [1], and also, in the case of lipophilic derivatives, in chlorinated organic solvents [2]. So far, this tetrameric arrangement has been the only basic structure found in gels [3], in columnar liquid-crystalline phases [1][4], in assembled structures of telomere model sequences [5], and in self-assembled species formed, in organic solvents, by 3′,5′-di-*O*-decanoyl-2′-deoxyguanosine (**1**) in the presence of alkaline picrates [2].

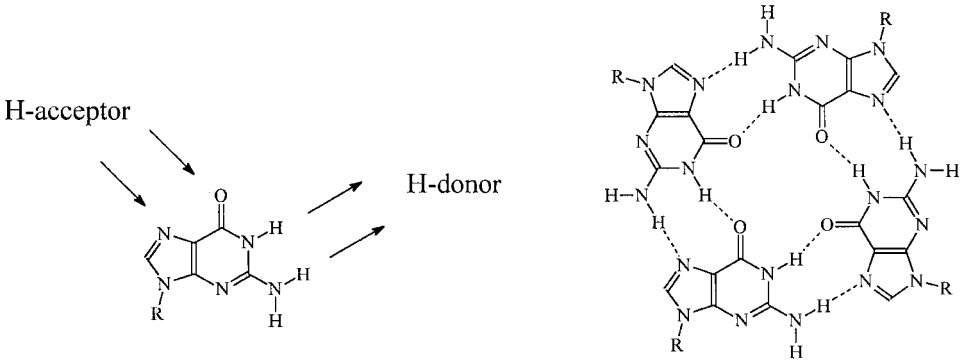

Fig. 1. *Cyclic* Hoogsteen *H-bonded quartet formed by four guanosine residues*

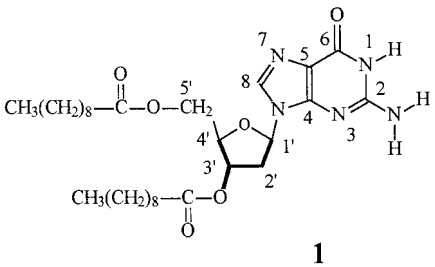

1

In the course of our work on lipophilic guanosines, we noticed that compound **1** in hydrocarbon solvents forms a gel-like phase, which, however, under microscopic observation, did not show the fibrillar structure typical of gels [6]. A preliminary X-ray diffraction analysis revealed instead the formation of a liquid-crystalline mesophase. We now describe an investigation on the self-assembly of deoxyguanosine **1**, starting from dilute solutions and gradually increasing the concentration to reach the liquid-crystalline state and finally the fibre state. In all cases, the aggregates result from a new H-bond pattern, completely different from the classical G-quartet.

2. The Self-Assembly Process. – 2.1. *^{1}H-NMR Data of* **1**. The ^{1}H-NMR data of derivative **1** were recorded in $CDCl_3$ (*Table 1* and *Fig. 2*). The assignments of the signals due to the deoxyribose moiety were achieved by a COSY experiment using standard methods.

In particular, the H–C(1′), H–C(2)′, H′–C(2′), H–C(3′), and H–C(4′) resonances of **1** were unambiguously assigned. The diastereotopic H–C(2′) and H′–C(2′) were both assigned on the basis of H–C(1′)/H–C(2′), H–C(1′)/H′–C(2′), and H–C(2′)/H–C(3′) NOE cross-peak intensities in NOESY spectra of $3.5 \cdot 10^{-2}$ and $6.3 \cdot 10^{-2}$ M solutions (mixing times 350–400 ms). Regardless of the sugar conformation, the *H*–C(1′)/*H*′–C(2′) and *H*–C(2′)/*H*–C(3′) interproton distances were always shorter than the *H*–C(1′)/*H*–C(2′) and *H*′–C(2′)/*H*–C(3′) distances, respectively. The H–C(3′)/H–C(4′) cross-peak was very weak due to the small *J* coupling constant. The H–C(2′) resonance falls downfield of that of H′–C(2′). The diastereotopic protons H–C(5′) and H′–C(5′) were not individually assigned.

Table 1. *^{1}H-NMR Data* ($CDCl_3$) *of* **1** ($3.20 \cdot 10^{-3}$ mol l^{-1} [a])

	δ/ppm	*J*(H,H)/Hz	T_1/s
H–C(8)	7.69 (*s*)		1.41 ± 0.03
H–C(1′)	6.23 (*dd*)	8.0, 6.2	1.03 ± 0.03
H–C(2′)	2.85 (*ddd*)	14.0, 8.0, 6.2	0.31 ± 0.02
H′–C(2′)	2.53 (*ddd*)	14.0, 6.2, 1.8	0.31 ± 0.02
H–C(3′)	5.39 (*m*)		0.81 ± 0.03
H–C(4′)	4.33 (*m*)		0.57 ± 0.02
H–C(5′)	4.41 (*dd*)	n.d.	0.36 ± 0.01
H′–C(5′)	4.38 (*dd*)	n.d.	0.40 ± 0.01
H–N(1)	12.14 (br. *s*)		1.83 ± 0.14
H_2N–C(2)	5.89 (br. *s*)		0.24 ± 0.01

[a]) Other resonances (*J* in Hz, T_1 in s): 2.37 (*t*, *J* = 7.1, T_1 0,68 ± 0.03, 1 CH_2CO); 2.35 (*t*, *J* = 7.1, T_1 0.66 ± 0.03, 1 CH_2CO); 1.61 (*m*, T_1 1.67 ± 0.10, 2 CH_2CH_2CO); 1.20–1.30 (*m*, T_1 1.24 ± 0.10, 24 H, CH_2); 0.89 (*t*, *J* = 6.5, T_1 2.28 ± 0.10, 1 Me); 0.87 (*t*, *J* = 6.5, T_1 2.28 ± 0.10, 1 Me).

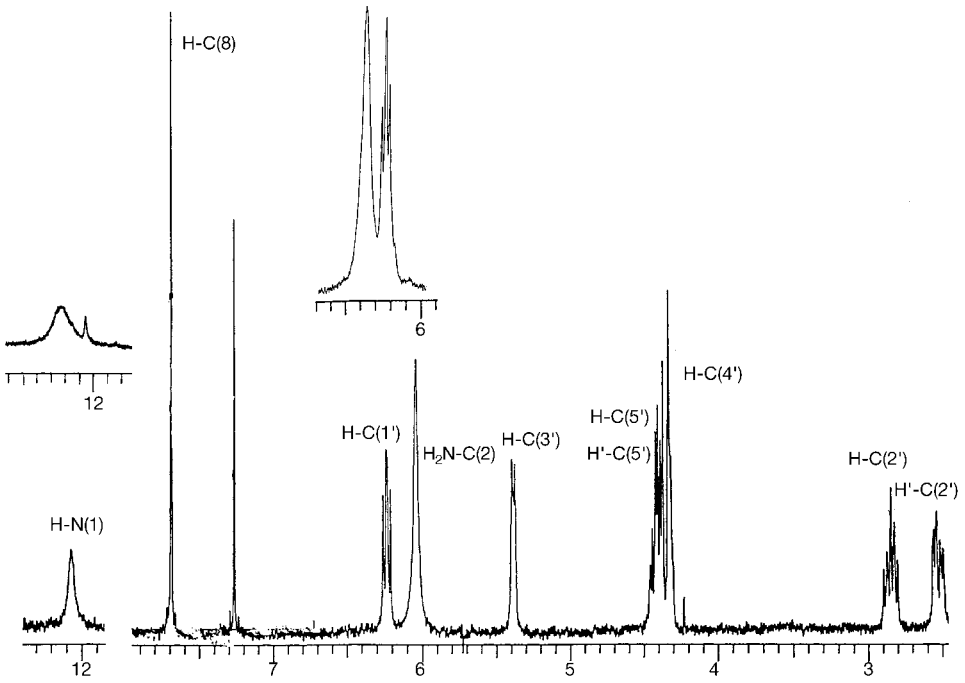

Fig. 2. *^{1}H-NMR Spectrum of a $3.80 \cdot 10^{-3}$ M solution of* **1** *in $CDCl_3$.* In the inset, two relevant parts of the spectrum of a $3.54 \cdot 10^{-2}$ M solution of **1** in $CDCl_3$ are shown.

2.2. *The Aggregate at Low Concentration.* The *s* due to the imino proton NH of **1**, is at *ca.* 12 ppm, a value typical for an H-bonded proton [7][8]. We are confident in this statement as, after complexation with K^+ ions and unambiguous formation of an octamer composed of two G-quartets, this signal moves slightly upfield [2]. It should be pointed out that the position of this peak does not change with concentration in the range $4 \cdot 10^{-4}$ to $3.5 \cdot 10^{-2}$ M, indicating complete association. In DMSO, the *s* is shifted to 10.7 ppm, as could be expected for a solvent in which solute-solute H-bonding is less favored. *Rich* and coworkers [9], from an IR study, reported an equilibrium constant in the range $10^3 - 10^4$ for G·G association in $CHCl_3$, in agreement with the present observations.

The H–C(8) signal is a *s* at *ca.* 7.7 ppm, and the two side signals, typical of structures formed by assembled G-quartets [2][10], are not detectable at low concentration values. The NH_2 signal appears below 6 ppm in the concentration range $4 \cdot 10^{-4}$ to $3.2 \cdot 10^{-3}$ M; furthermore, the absence of enhancements at the NH signal, on irradiation of the NH_2 signal in one-dimensional NOE experiments in such solutions also suggests a free NH_2 group. Below it will be shown that in concentrated solutions, where the NH_2 group becomes involved in cyclic H-bonds, the enhancement is instead present (see *Chapt. 2.3*).

The chemical-shift data and the absence of NOE interaction imply that, in $CDCl_3$, deoxyguanosine **1** is self-associated, and the proton NH is involved in H-bonding, while NH_2 is not: the cyclic dimer **2** seems the obvious choice. Curiously, several years ago,

Nash and *Bradley* [11] calculated that, *in vacuo*, this dimer is the most stable of the possible guanine dimers; recent calculations [12] confirm that this is in fact the most stable dimer[1]).

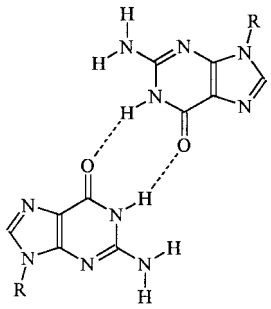

2

The CD spectrum of **1** in $CDCl_3$ is weak and does not show exciton patterns, indicating that the two guanine chromophores are in a non-coupling geometry, as shown in the planar dimer **2**.

The existence of a dimer (and of a trimer, see *Chapt. 2.3*) is confirmed by electrospray ionization mass spectrometry (ESI-MS). This technique has recently been extended to the characterization of aggregates containing non-covalent interactions [14]. It has been shown that ESI-MS can provide an image of the supramolecular species present in the solution [15]. Thus, deoxyguanosine **1** was analyzed by ESI-MS in the positive-ion mode: the spectrum (*Fig. 3*) clearly shows the presence of a protonated dimer $[2M+H]^+$ whose abundance is *ca.* 50% of that of the protonated monomer $[M+H]^+$[2]).

2.3. *The Aggregates at Medium to High Concentration*. As shown in *Table 2*, the situation is not static, and new events occur in more concentrated $CDCl_3$ solutions of **1** or at low temperature. The NH_2 signal moves downfield on increasing the concentration of **1**, suggesting that also this group becomes progressively engaged in H-bonding[3]). Furthermore, the spectrum of a $3.5 \cdot 10^{-2}$ M solution of **1** at room temperature shows broadening of the NH signal centred at 12.2 ppm[4]). These results indicate new self-assembled species which are present in consistent amounts also at room temperature in highly concentrated solutions. The dimeric form and the new assembled species are likely to be present, at room temperature, in a fast-exchange regime.

---

[1]) The possible formation of guanosine dimers also in DMSO was considered by *Newark* and *Cantor* [13].

[2]) Also 2′,3′,5′-tri-*O*-acetylguanosine yields, in the same solvents, the protonated dimer $[2M+H]^+$ in a considerable amount (*ca.* 50% of $[M+H]^+$).

[3]) Also on lowering the temperature of a *ca.* $4 \cdot 10^{-3}$ M solution of **1**, the NH_2 chemical shift increases, and the signal becomes broad and disappears at $-45°$; meanwhile, also the NH signal becomes broad and shifts towards slightly higher chemical shifts (down to *ca.* 12.3 ppm).

[4]) At this concentration, also a second small signal appears at *ca.* 12.06 ppm, the δ of the octamer formed by two G-quartets; this attribution is confirmed by the presence of the two side-signals of H–C(8) which characterize the octamer [2].

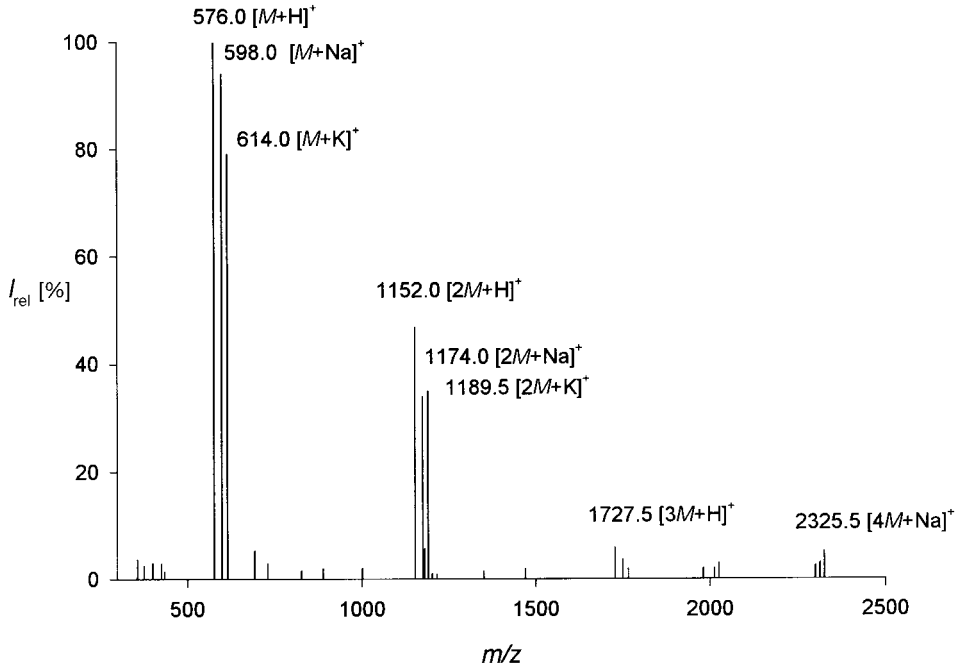

Fig. 3. *ESI-MS of* **1** *in acetone* (for details, see *Exper. Part*)

Table 2. *^{1}H-NMR Chemical Shifts of NH_2–C(2) of* **1** *in $CDCl_3$ as a Function of Concentration*

[**1**]/mol l^{-1}	$4.35 \cdot 10^{-4}$	$9.56 \cdot 10^{-4}$	$3.20 \cdot 10^{-3}$	$3.80 \cdot 10^{-3}$	$1.35 \cdot 10^{-2}$	$3.54 \cdot 10^{-2}$	$6.35 \cdot 10^{-2}$
δ/ppm	5.60	5.72	5.89	6.04	6.13	6.37	6.46

To get more information about the structure of this second self-associated species, some steady-state NOE and NOESY experiments were performed. Both sets of experiments, carried out at room temperature with $(1-6.3) \cdot 10^{-2}$ M solutions[5]), show negative enhancements or positive cross-peaks, indicating that deoxyguanosine **1** behaves as a large molecule with $M_r > 1000$ ($\omega\tau_c > 1$). These experiments allow the detection of an important new interaction between the NH_2 group and the NH proton at 12.27 ppm. This NOE, obtained at high concentration, together with the shift of the NH_2 resonance, indicates that also the NH_2 group becomes involved in H-bonding, even if, in $CDCl_3$, the equilibrium constant of this process is likely to be small. Considering that the association described previously (dimer **2**) seems to be complete under all the conditions employed for recording the spectra, only two H-bond acceptors remain available, N(3) and N(7). *Jorgensen* and coworkers [12] have calculated the interaction energy for a cyclic dimer in which N(3) is involved (-10.8 kcal mol^{-1}). Thus, we propose structure **3** for the second self-associated species (*Fig. 4*). The equilibrium constant for dimer **3** should be about half that of dimer **2**, but certainly non-negligible. A similar pairing between guanines moieties has recently been reported by

[5]) The NOE experiment carried out at $-45°$ and with $c = 4 \cdot 10^{-3}$ M, shows intense spin-diffusion effects.

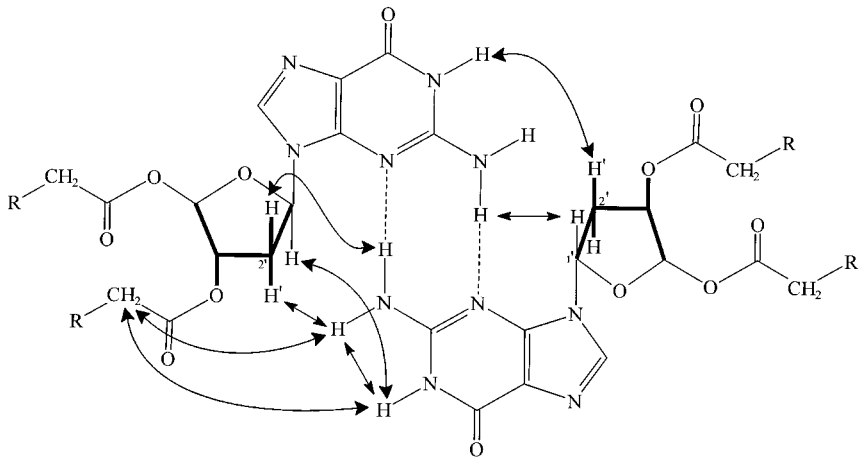

3

Fig. 4. *Cyclic dimer* **3** *involving N(3) and the exocyclic NH_2 group.* The observed NOE interactions are indicated by arrows.

Wang and coworkers [16] for parallel-stranded *Π*-DNA-formed by G-A rich-oligonucleotides[6]).

Structure **3** can explain the NOE interaction (not observed in dilute solutions) between the NH_2 and NH protons which is likely to originate from prevented rotation around the NH_2–C(2) bond due to the formation of the cyclic H-bond system [7]. Other steady-state NOE experiments indicate indirectly that the NH_2 group is H-bonded to N(3).

Thus, saturation of H–C(2′) and H′–C(2′) of the deoxyribose moiety of **3** causes the enhancement of the NH_2 signals, saturation of H–C(1′) and H′–C(2′) induces enhancement of the NH_2 and NH signal, and irradiation at the resonance of the $CH_2(\alpha)$ protons of the 3′-*O*-decanoyl group leads to the enhancement of the NH_2 and NH signals[7]). These results confirm the proximity between the NH_2 group of one molecule and the sugar protons of another molecule. The interaction between $CH_2(\alpha)$ and NH_2 further confirms the model.

A final support to the assembly scheme proposed comes from the ESI-MS (*Fig. 3*) where a weak signal (*ca.* 5% of $[2M+H]^+$) corresponding to a trimer could be detected in the accessible range of our instrumentation. Its weak intensity is likely to be connected to the lower stability of the cyclic H-bonding of **3**. Accordingly, the adenosine analogue, 2′,3′,5′-tri-*O*-acetyladenosine, gives only a small amount of the dimeric ion (less than 5%).

A probable assembled structure, obtained after inspection of CPK models and computer modelling, is sketched in *Fig. 5*. It should be noticed that the assembly of *Fig. 5* is possible only if all the deoxyguanosines are disposed with the same of the two nonequivalent faces on the same side of the ribbon; the two faces of the ribbon are by no means equivalent. In this structure, each molecule forms H-bonds with only two

---

6) We thank a referee for this reference.

7) The signals of $CH_2(\alpha)$ of the chains at C(3′) and C(5′) are not completely resolved; however, in the model, the $CH_2(\alpha)$ at C(5′) is far away from the NH_2 group, while that at C(3′) is close.

neighboring molecules, and the H-bonds between two molecules form a cyclic eight-membered ring, a classic scheme that permits the formation of tapes [17]. A ribbon-like motif was reported in the crystal structure of 2′,3′,5′-tris-*O*-[(*tert*-butyl)dimethylsilyl]-guanosine [18]; this ribbon is again formed by an H-bond network which involves also a molecule of methanol. Also 2′,3′-*O*-isopropylidene-5′-*O*-[(*tert*-butyl)dimethylsilyl]isoguanosine forms, in the crystal, a ribbon-like structure involving a H-bond scheme very similar to that reported in *Fig. 5* [19]: there is an amide-amide cyclic coupling and the exocyclic 6-amino groups are bonded to the nearby N(7) in a cyclic form. Very recently, *Lehn* and coworkers [20] have reported a crystal structure with supramolecular pyrimidinediamine ribbons where pyrimidinediamines are interconnected *via* two sets of H-bonds; one of the two sets is of the α-aminopyridine-dimer type equivalent to that proposed for **3**.

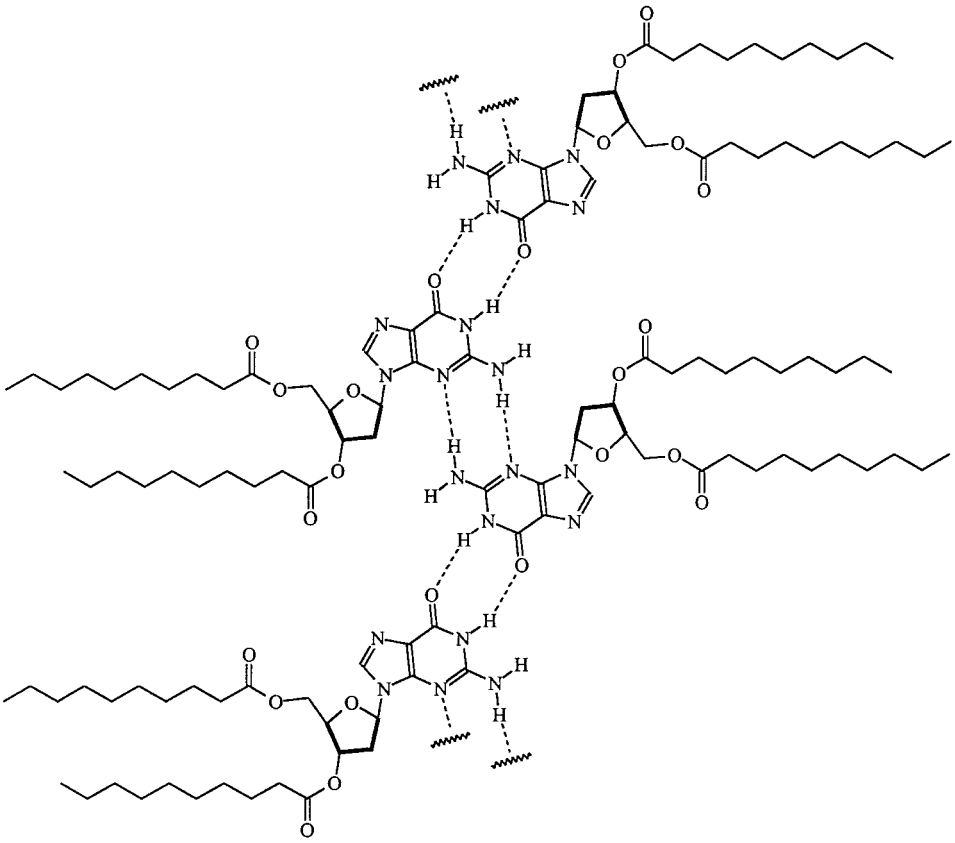

Fig. 5. *H-Bond pattern of the ribbon-like assembled structure of* **1**

To obtain information on the assembled species present in hydrocarbon solvents, we measured IR spectra in the region of the NH_2 and NH stretching frequencies (3600–3200 cm^{-1}) in both $CDCl_3$ and hexadecane (*Fig. 6*). In none of the spectra, a band at *ca.* 3385 cm^{-1} is observable; this frequency is reported to correspond to the free NH stretching for inosine [9] and 1-cyclohexyl-5-bromouracil [21]. Only the spectrum of

the dilute solution in $CDCl_3$ (*Fig. 6,a*) shows the two bands at *ca.* 3515 and 3409 cm^{-1}, corresponding to the free NH_2 of guanine [22]; in addition, even for this concentration, bands corresponding to the bonded NH_2 are present. In the more concentrated solution (*Fig. 6,b*), only the more intense component at *ca.* 3409 cm^{-1} is still visible, and in hexadecane at the same concentration (*Fig. 6,c*), no trace of the two bands is left. The IR data are in excellent agreement with the H-bonding situation deduced from the ^{1}H-NMR spectra. Furthermore, the spectrum of the liquid-crystalline phase in hexadecane, a solvent where solute-solute intermolecular H-bonds should be favored, shows only fully bonded species, even at relatively low concentration. Although the detailed structural information was deduced from NMR spectra in $CDCl_3$, the IR data in hexadecane are in agreement with the structure depicted in *Fig. 5*, and there seems to be no relevant reason to think of different assembled species.

From spectroscopic studies, one can conclude that, in dilute $CDCl_3$ solutions at room temperature, dimer **2** is the main species. At higher concentrations and/or at

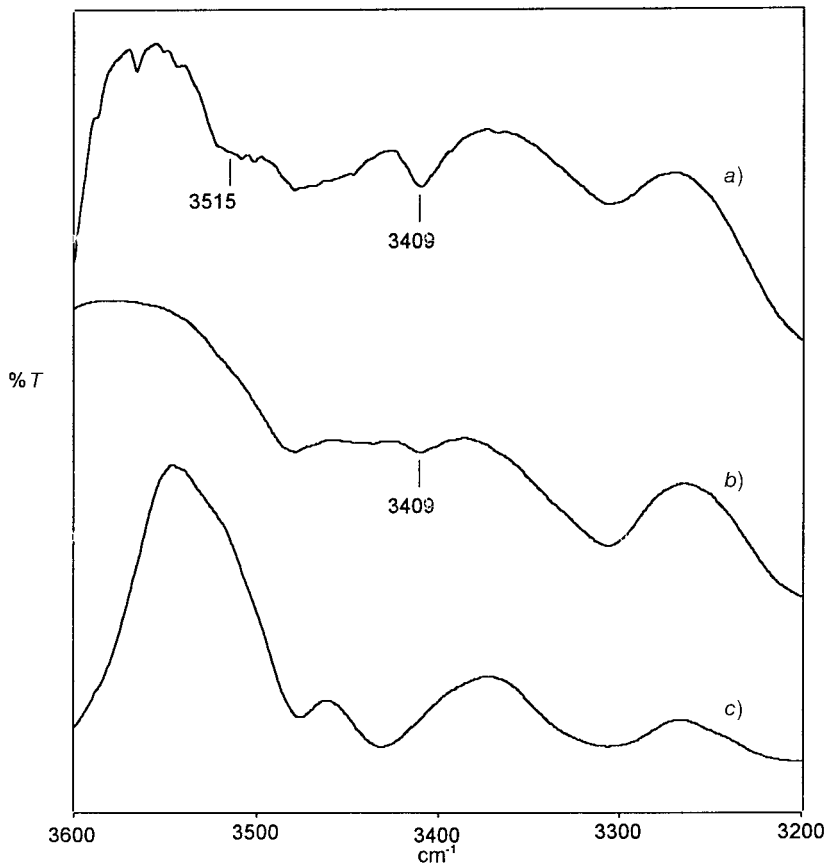

Fig. 6. *IR Spectra of deoxyguanosine* **1** a) *in $CDCl_3$ at a concentration of $2.5 \cdot 10^{-3}$* M (path length 5 mm), b) *in $CDCl_3$ at a concentration of $7.0 \cdot 10^{-2}$* M (path length 3 mm), *and* c) *as liquid-crystalline phase formed in hexadecane at a concentration of $7 \cdot 10^{-1}$* M (path length 2 mm)

lower temperatures, extended structures of the type depicted in *Fig. 5* begin to be relevant; they become the dominant species in hydrocarbon solvents where the liquid-crystalline phase is observed. These structures are very likely to be the building blocks of the mesophase.

3. The Aggregate in the Solid State: the Structure of the Fibre. – In the NMR tubes, after slow evaporation of the solvent, large crystal-like platelets were observed which could be collected and used for X-ray diffraction measurements. In preliminary measurements at very high angles on a single-crystal apparatus, no diffraction peaks were observed, indicating a highly disordered system. Measurements with a *Guinier*-type X-ray camera confirmed the non-crystalline structure of the sample, suggesting a fibre-like organization with long periodicity. In particular, X-ray diffraction experiments were performed both on powder samples (obtained by crushing the platelets) and on single platelets; however, no oriented diffraction pattern was obtained. A typical diffraction profile is shown in *Fig. 7*. Four very broad peaks characterize the low-angle region: as indicated in *Fig. 7* and reported in *Table 3*, these peaks can be indexed according to a lamellar one-dimensional lattice, $s_{h,0} = h/d$ ($h = n$, n integer), where d is the lamellar unit cell, h,0 are the *Miller* indices of the reflection, and s is the module of the vector specifying the position of the lattice points in the reciprocal space ($s = (2\sin\theta)/\lambda$, 2θ being the scattering angle and λ the X-ray wavelength). A lamellar-like layer structure, with a unic cell of 30.9 Å, is then deduced. From the width of the (h,0) *Bragg* peaks, a correlation length of *ca.* 100 Å was calculated; this very short correlation length (only three times the unit-cell dimension) is indicative of a very poor correlation in the packing of the layers.

Further indications about the fibre structure were obtained from the other features which characterize the X-ray diffraction profile: *i*) A very diffuse band is observed at *ca.* 4.2 Å. In liquid paraffines, as well as in anhydrous surfactant mesophases, where the

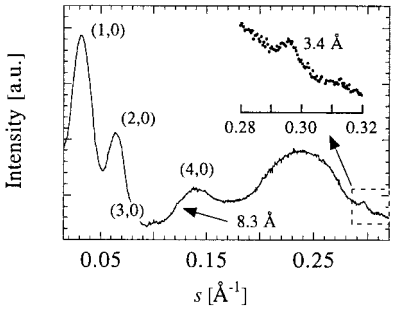

Fig. 7. *X-Ray diffraction profiles obtained at 25° from the platelets obtained after slow evaporation of chloroform solutions*

Table 3. *Indexing of the Experimental X-Ray Low-Angle Diffraction Pattern Observed in the Fibre. s* (in $Å^{-1}$) is the reciprocal spacing of the reflection with *h,k Miller* indices; obs. refers to the observed spacings, while calc. refers to those calculated for the selected space group, 1-D, $d = 30.9$ Å.

h,k	1,0	2,0	3,0	4,0
$S_{obs.}$	0.0324	0.0648	0.0970	0.1293
$S_{calc.}$	0.0324	0.0647	0.0971	0.1294

hydrocarbon chains assume a liquid-like conformation, X-ray diffraction diagrams are characterized by a similar diffuse band in this position [23]. *ii*) A narrow peak is observed at $s = (3.4\ \text{Å})^{-1}$. According to previous results from guanosine columnar lyotropic phases [24], this peak is indicative of guanine stacking, *i.e.*, of the regular piling of guanine residues one on top of the other. *iii*) A low-intensity diffraction peak is detected at $s = (8.3\ \text{Å})^{-1}$. This peak could be related to a (lateral) correlation inside the layers. In the absence of oriented diffraction data, a more detailed interpretation could not be given.

According to X-ray data and in analogy to the self-organized structures observed in amphiphilic surfactants and lipids, where polar and nonpolar groups aggregate separately, the fibre can be conveniently described as a lamellar-like assembly (see *Fig. 8*) in which the guanine residues and the alkyl chains form separate layers. Considering the 3.4-Å peak and the extensive self-assembly detected in dilute solution, the base layer can be described as composed of the ribbon-like aggregates (*Fig. 8,a*), lined on each side and stabilized by the stacking interactions between guanine moieties packed at a 3.4-Å distance (*Fig. 8,b*). The origin of the 8.3-Å peak can also be deduced: it should be related to the lateral repeat distance between the guanine residues in the lined ribbons. Moreover, the diffuse 4.2-Å band indicates that the decanoyl chains, which form the paraffinic layers (*Fig. 8,c*), adopt a disordered conformation. The proposed structure also accounts for the experimental layer dimension: as evaluated from molecular models, the layer thickness calculated, assuming for the hydrocarbon chains a fully extended conformation, is *ca.* 35 Å. This value is slightly higher than the experimental unit cell (30.9 Å), in agreement with the disordered arrangement adopted by the alkyl chains in the fibre. Moreover, some interdigitation is likely to be present.

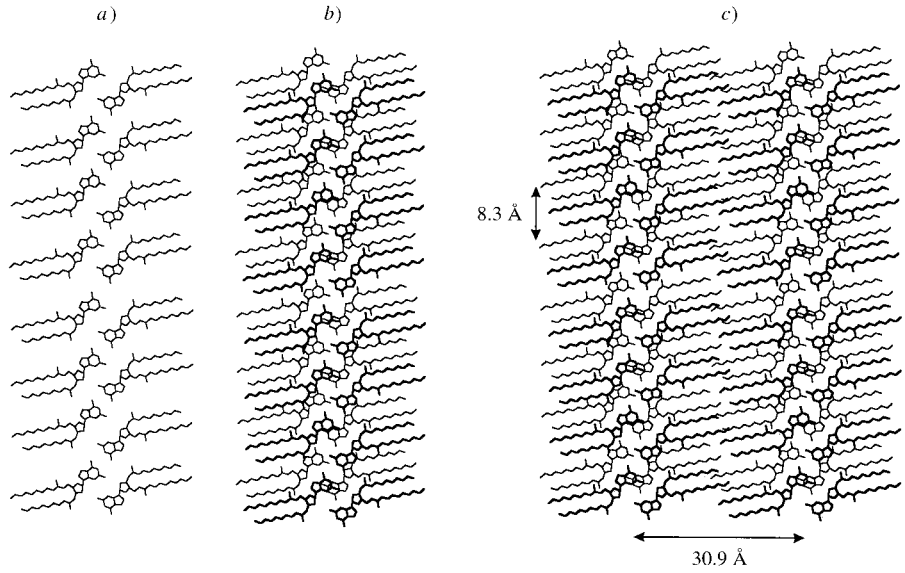

Fig. 8. *Picture* a) *of a ribbon*, b) *of the stacking of two ribbons, and* c) *of the lamellar-like structure of the fibre with distances obtained from X-ray diffraction*. The H-bonds between the guanines are omitted but are as depicted in *Fig. 5*.

To assess this conclusion, modelling of the possible arrangement of two tapes formed by four monomers was carried out on 3′,5′-di-*O*-acetyl-2′-deoxyguanosine (acetic instead of decanoic acid esters were used for simplicity; for details, see *Exper. Part*): the results are shown in *Fig. 9*. Each guanine ribbon displays the extended array of H-bonds illustrated in *Fig. 5* and suggested by the experimental ^{1}H-NMR data. The two deoxyguanosine layers are assembled in such a way that the guanine ribbons lie on parallel planes at the distance of *ca*. 3.4 Å, and the sugar moieties with their lipophilic chains point outwards from the core of the ribbons. The tapes are shifted one with respect to the other along the longitudinal axis and give rise to two parallel sequences of deoxyribose fragments, from which the lipophilic chains depart. This molecular arrangement shows that the guanine ribbons become tightly packed, placing the atoms at the *van der Waals* distance and free of unfavorable contacts, *i.e.*, void space in the solid is minimized by parallel alignment of the tapes that pack in a manner that permits the interdigitation of substituents on adjacent tapes.

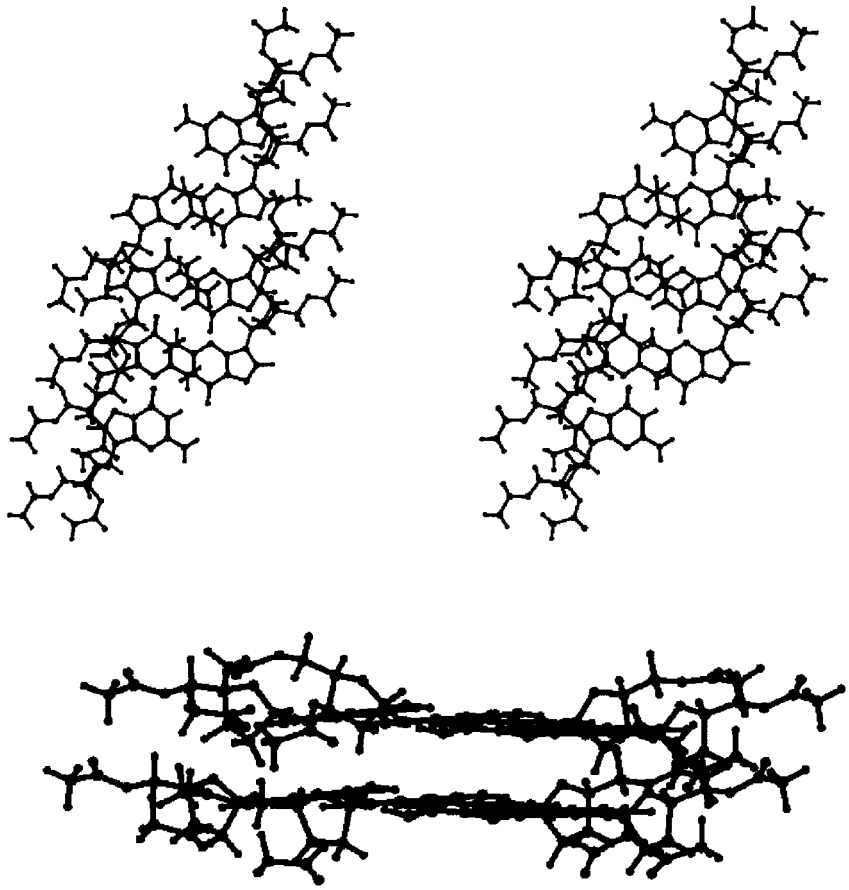

Fig. 9. *Stereoplot of a possible spatial arrangement of two tetramers of 3′,5′-di-*O*-acetyl-2′-deoxyguanosine.* Each of the two guanine strands is stabilized by intermolecular H-bonds, and the corresponding planes are 3.4 Å apart.

4. The Liquid-Crystalline Phase. – When deoxyguanosine **1** is dissolved in the minimum amount of CH_2Cl_2 or $CHCl_3$, and hexane, heptane, or hexadecane is added, a biphasic system or a compact birefringent gel-like phase is observed according to the amount of solvent. The use of a chlorinated solvent is necessary due to the very low solubility of solid **1** in hydrocarbons. When using hexadecane, it is possible to remove all the chlorinated solvent. This operation does not, however, affect the gel-like phase: no crystallization or modification of the microscopic texture are observed even after several months. The molecular mass of the hydrocarbon used as solvent does not seem to affect the texture of the phase. In hexadecane, the biphasic system is first observed at *ca.* 1% (*w*/*w*), and the pure gel-like phase is present between 8 and 10% (*w*/*w*). Above 10% (*w*/*w*), the gel-like phase appears to coexist with the solid. In no cases, the fibrillar structures typical of many gels can be observed [6]. The microscopic observation seems to be in favor of a liquid-crystalline phase rather than of an anisotropic gel.

A preliminary X-ray investigation indicates a liquid-crystalline phase whose building blocks are the ribbon-like aggregates described above. The structure of the phase will be reported in a separate communication.

5. Conclusions. – Spectroscopic investigations indicate that in chlorinated solvents and, to a large extent, in hydrocarbons, deoxyguanosine **1** undergoes extensive self-assembly to give structures whose core is a planar ribbon-like array of H-bonded guanine moieties (*Fig. 5*). X-Ray diffraction of the platelets obtained from $CHCl_3$ indicates a fibre composed of stacks of the ribbon-like aggregates. Preliminary X-ray diffraction of the gel-like phase in hydrocarbon solvents shows a liquid-crystalline order.

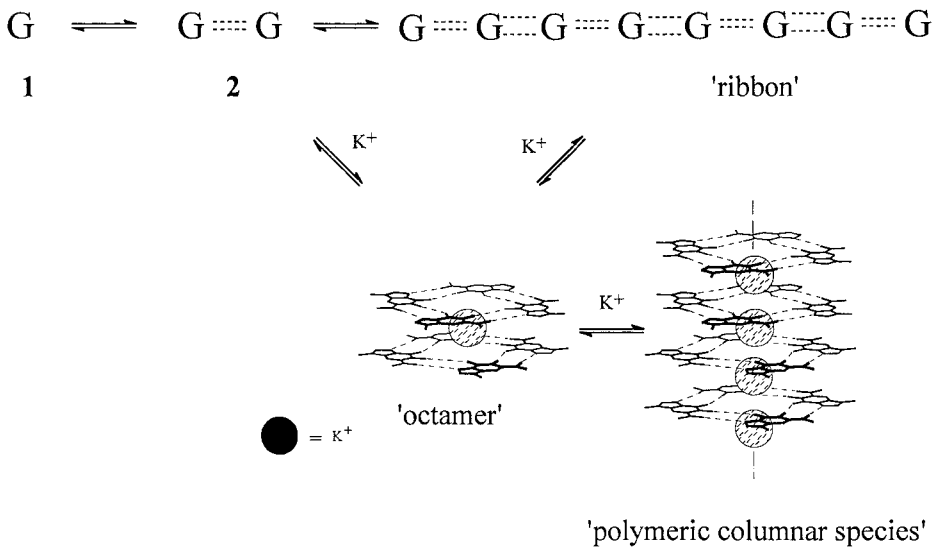

Fig. 10. *Schematic representation of the dimeric* (**2**) *and polymeric* ('ribbon') *aggregates of deoxyguanosine* **1**. The double dotted lines indicate strong (::::::) and weak (::::::) double H-bonds, respectively. In the presence of K^+, octamers or polymeric aggregates are formed, according to the amount of K^+ added.

Lipophilic deoxyguanosine **1** is a versatile molecule which can form different self-assembled structures depending on the experimental conditions, as depicted in *Fig. 10*. In $CHCl_3$, it is assembled as the dimeric or polymeric form, at low or high concentration, respectively. In the presence of K^+ ions, these forms are converted into octamers, based on G-quartets [2]. By further addition of K^+ ions, the octamers are transformed into polymeric columnar species, based again on G-quartets [2].

We would like to thank Dr. *Jeffery T. Davis*, University of Maryland, for stimulating discussions and criticism and for providing the crystal structure of 2′,3′-*O*-isopropylidene-5′-*O*-[(*tert*-butyl)dimethylsilyl]isoguanosine. We are grateful to Prof. *D. Braga* and Dr. *F. Grepioni*, Bologna, for high-angle X-ray measurements and useful comments. *NATO* is gratefully acknowledged for a collaborative research grant (SRG 960583). We thank *MURST* (Italy, Program 'Liquid Crystals: Structures, Computer Simulations, Properties and Applications'), *CNR* (Italy), and the University of Bologna (funds for selected research topics 1995–97) for financial support.

Experimental Part

Synthesis of **1**. 2′-Deoxyguanosine monohydrate (*Fluka*) was converted into 2′-deoxy-N^2-[(9*H*-fluoren-9-ylmethoxy)carbonyl]guanosine ($Fmoc^2G_d$) according to the procedure described by *Koole et al.* [25]. $Fmoc^2G_d$ (1.00 g, 2.04 mmol) was co-evaporated with dry pyridine (3 × 5 ml) and finally dissolved in dry pyridine (30 ml). To the clean soln. thus obtained were added dropwise 2.3 ml (11 mmol) of decanoyl chloride, and the resulting mixture was allowed to react for 2 h. MeOH (2 ml) was then added, and stirring was continued for 15 min. Then sat. $NaHCO_3$ (50 ml) was added, and the mixture was extracted with CH_2Cl_2 (3 × 20 ml). The combined org. phase was washed with H_2O (10 ml), dried (Na_2SO_4), and evaporated and the oily residue co-evaporated with toluene (3 × 20 ml) and purified by column chromatography (silica gel, CH_2Cl_2/MeOH 98:2): *3′,5′-di*-O-*decanoyl-2′-deoxy*-N^2-*[(9*H*-fluoren-9-ylmethoxy)carbonyl]guanosine* (75% yield) as whitish foam. ^{1}H-NMR (300 MHz) $\delta(CDCl_3)$: 0.90 (*m*, 2 Me); 1.29 (*m*, 12 CH_2); 1.61 (*m*, 2 CH_2CH_2CO); 2.35 (*m*, 2 CH_2CH_2CO); 2.52 (*m*, 1 H–C(2′)); 2.95 (*m*, 1 H–C(2′)); 4.22 (*t*, CH (Fmoc)); 4.35 (*d*, CH_2 (Fmoc)); 4.52 (*m*, H–C(4′), 2 H–C(5′)); 5.39 (*m*, H–C(3′)); 6.20 (*m*, H–C(1′)); 7.72–7.75 (*m*, 8 H (fluorene)); 7.81 (*s*, H–C(8)); 9.25 (br. *s*, NH); 11.4 (br. *s*, NH).

To a soln. of 3′,5′-di-*O*-decanoyl-2′-deoxy-[N^2-[(9*H*-fluoren-9-ylmethoxy)carbonyl]guanosine (0.50 g, 0.62 mmol) in CH_2Cl_2 (12 ml), piperidine (2.0 ml) was added. The mixture was stirred for 30 min and then washed with sat. NH_4Cl soln. (20 ml) and H_2O (20 ml). The org. phase was dried (Na_2SO_4) and evaporated and the residue purified by column chromatography (silica gel, CH_2Cl_2/MeOH 97:3): *3′,5′-di*-O-*decanoyl-2′-deoxyguanosine* (**1**; 65% yield) as a glassy non-hygroscopic colorless solid. M.p. (DSC) at *ca.* 165° (with low enthalpy) and decomposition at *ca.* 210°. ^{1}H-NMR (300 MHz): *Table 1*. ^{13}C-NMR (75.45 MHz, $CDCl_3$): 173.50, 173.12 (O–C=O); 158.96 (C(6)); 152.81 (C(2)); 151.22 (C(4)); 135.66 (C(8)); 117.35 (C(5)); 84.26 (C(1′)); 82.50 (C(4′)); 74.40 (C(3′)); 63.67 (C(5′)); 37.20 C(2′)); 34.08, 34.01, 31.80, 29.36, 29.27, 29.24, 29.22, 29.09, 29.06, 24.76, 22.61 (CH_2); 14.06 (Me).

Preparation of the Liquid-Crystalline Phase. The liquid-crystalline phase was prepared by dissolving **1** (in a typical experiment, 30 mg) in the chlorinated solvent CH_2Cl_2 or $CHCl_3$ (0.4 ml) and adding the relevant amount of hydrocarbon solvent hexane, heptane, or hexadecane (0.35–4 ml). When the hydrocarbon solvent was hexadecane, the chlorinated solvent was removed under vacuum. The absence (< 2%) of residual chlorinated solvent was checked by GC.

X-Ray Diffraction. Low-angle X-ray diffraction experiments were performed using a 3.5-kW *Philips-PW1830* X-ray generator equipped with a *Guinier*-type focusing camera operating in vacuum: a bent quartz crystal monochromator was used to select the Cu-$K_{\alpha 1}$ radiation (λ 1.54 Å). The samples were mounted in vacuum-tight cells with thin mica windows. To reduce the spottiness arising from possible macroscopic monodomains, the cells were continuously rotated during exposure. The sample-cell temp. was controlled with an accuracy of 0.5° by using a circulating thermostat. The diffraction patterns were recorded on a stack of four *Kodak-DEF-392* films.

NMR Measurements. ^{1}H- an ^{13}C-NMR Spectra: at 300 and 75.45 MHz, respectively, with a *Varian-Gemini-300* instrument, δ(H) in ppm from the solvent peak in $CDCl_3$ solns. and coupling constants J in Hz; δ(H) for $4.35 \cdot 10^{-4}$ to $6.3 \cdot 10^{-2}$ M solns. 2D-COSY: $3.5 \cdot 10^{-3}$ M soln. *Varian-Gemini-200* instrument, spectral width 3 kHz, pulse width 25 μs (90° flip angle), relaxation delay 4 s, complex data points in t_1 1024, complex FIDs in t_2 256,

number of repetitions 16. Low-temperature (10 to $-45°$) ^{1}H-NMR spectra: $4 \cdot 10^{-3}$ M soln. 1D-NOE Steady-state difference experiments and phase-sensitive 2D-NOESY spectra: $2.5 \cdot 10^{-3}$ to $-6.3 \cdot 10^{-2}$ M and $(1-6.3) \cdot 10^{-2}$ M solns., resp. Steady-state NOE measurements: *Varian-Gemini-300* spectrometer; a number of transients (160–320) were accumulated using relaxation delays of 2–4 s and a minimum decoupler power to obtain NOE signals. The instrumental settings of the 2D-NOESY experiments were: spectral width 4.5 kHz, pulse width 11 μs (90° flip angle), repetition time 3 s, complex data points in t_1 1024, complex FIDs in t_2 256, mixing times τ_m 0.35–0.5 s, number of transients 16.

Circular Dichroism and IR Spectra. Circular dichroism and absorption spectra: *Jasco-J-710* spectropolarimeter. IR Spectra: *Perkin-Elmer-1600-FT-IR* spectrometer using *Perkin-Elmer* variable path length cells.

ESI-MS Measurements. Spectra were obtained in MeCN or 1,2-dichloroethane with a *VG-Trio-2000* instrument (*Fisons*) or in acetone with a *PE-Sciex* triple quadrupole instrument (courtesy of Dr. *J. T. Davis*); no special care was taken to eliminate traces of alkali-metal ions. Their presence is also evident in NMR spectra at high concentration where small amounts of the octamer could be detected (see *Footnote 4*). This species is formed only in the presence of alkali-metal ions [2].

Molecular Modelling. The core of four H-bonded guanines was built using standard library fragments, and its geometry was optimized by means of the semi-empirical SCF-MO method AM1 (keywords MMOK, PRECISE) [26]. The structure obtained in this way reproduces the array of intermolecular H-bonds suggested by the NMR experiments, and the relative positions of all the tetramer atoms were kept constant in the subsequent modelling procedure. The 3′,5′-di-*O*-acetyl-2′-deoxyribose moieties were then added in the proper positions, and an assembly of two of the resulting 3′,5′-di-*O*-acetyl-2′-deoxyguanosine tetramers was attempted. The determination of the mutual orientations of the guanine cores and the positioning of the sugar fragments and their ester substituents were initially carried out by a manual docking routine, checking the intermolecular energy of interaction between the pair of tetramers. When an arrangement was obtained corresponding to a distance of *ca*. 3.4 Å between the average planes containing the N- and the O-atoms of the guanine layers, the whole structure was energy-optimized (*in vacuo*, $\varepsilon = 1$) using the OPLS molecular-mechanics force field [27]. During the minimization (1000 steps), the positions of the guanine atoms were constrained by applying an energy penalty force constant of 1000 kJ/Å^2 mmol^{-1}. In the final model (*Fig. 9*), the distance between the guanine tetramers was 3.44 Å.

REFERENCES

[1] G. Gottarelli, G. P. Spada, A. Garbesi, in 'Comprehensive Supramolecular Chemistry', Eds. J. L. Atwood, J. E. D. Davies, D. D. MacNicol, F. Vögtle, J.-M. Lehn, J.-P. Sauvage, and M. W. Hosseini, Elsevier, Oxford, 1996, Vol. 9, p. 483.

[2] G. Gottarelli, S. Masiero, G. P. Spada, *J. Chem. Soc., Chem. Comm.* **1995**, 2555.

[3] S. Arnott, R. Chandrasekaran, C. A. Martila, *Biochem. J.* **1974**, *141*, 537; S. B. Zimmermann, D. R. Cohen, D. R. Davis, *J. Mol. Biol*. **1975**, *92*, 181; W. Guschlbauer, J. F. Chantot, D. Thiele, *J. Biomol. Struct. Dyn.* **1990**, *8*, 491.

[4] G. Gottarelli, G. Proni, G. P. Spada, *Enantiomer* **1996**, *1*, 201.

[5] D. Sen, W. Gilbert, *Biochemistry* **1992**, *31*, 65.

[6] Y. C. Lin, B. Kchar, R. G. Weiss, *J. Am. Chem. Soc.* **1989**, *111*, 5542; M. Aoki, K. Nakashima, H. Kawabata, S. Tsutsui, S. Shinkai, *J. Chem. Soc., Perkin Trans. 2* **1993**, 347.

[7] F. W. Smith, J. Feigon, *Nature (London)* **1992**, *356*, 164.

[8] Y. Kuroda, J. M. Lintuluoto, H. Ogoshi, *J. Chem. Soc., Perkin Trans. 2* **1997**, 333.

[9] Y. Kyogoku, R. C. Lord, A. Rich, *Biochim. Biophys. Acta* **1969**, *179*, 10.

[10] E. Bouhoutsos-Brown, C. L. Marshall, T. J. Pinnavaia, *J. Am. Chem. Soc*. **1982**, *104*, 6576.

[11] H. A. Nash, D. E. Bradley, *J. Chem. Phys.* **1966**, *45*, 1380.

[12] J. Pranata, S. G. Wierschke, W. L. Jorgensen, *J. Am. Chem. Soc*. **1991**, *113*, 2810.

[13] R. A. Newmark, C. R. Cantor, *J. Am. Chem. Soc.* **1968**, *90*, 5010.

[14] For a recent review, see M. Przybylski, M. O. Glocker, *Angew. Chem., Int. Ed. Engl*. **1996**, *35*, 806.

[15] E. Leize, A. Jaffrezic, A. Van Dorsselaer, *J. Mass. Spectrom*. **1996**, *31*, 537.

[16] H. Robinson, J. H. van Boom, A. H. J. Wang, *J. Am. Chem. Soc.* **1994**, *116*, 1565.

[17] S. Palacin, D. N. Chin, E. E. Simanek, J. C. MacDonald, G. M. Whitesides, M. T. McBride, G. T. R. Palmore, *J. Am. Chem. Soc*. **1997**, *119*, 11807.

[18] K. Araki, M. Abe, A. Ishizaki, T. Ohya, *Chem. Lett*. **1995**, 359.

[19] J. T. Davis, University of Maryland, unpublished results.

[20] M. Suarez, N. Branda, J.-M. Lehn, A. Decian, J. Fischer, *Helv. Chim. Acta* **1998**, *81*, 1.
[21] Y. Kyogoku, R. C. Lord, A. Rich, *Proc. Natl. Acad. Sci. U.S.A.* **1967**, *57*, 250.
[22] Y. Kyogoku, R. C. Lord, A. Rich, *Science* **1966**, *154*, 518.
[23] V. Luzzati, in 'Biological Membranes', Ed. D. Chapman, Academic Press, London, 1968, pp. 71 – 123.
[24] G. Gottarelli, G. P. Spada, P. Mariani, in 'Crystallography of Supramolecular Compounds', Eds. G. Tsoucaris, J. L. Atwood, and J. Lipkowski, Kluwer Academic Publ., Dordrecht, 1996, pp. 307 – 330.
[25] L. H. Koole, H. M. Moody, N. L. H. L. Broeders, P. J. L. M. Quaedflieg, W. H. A. Kuijpers, M. H. P. van Genderen, A. J. J. M. Coenen, S. van der Val, H. M. Buck, *J. Org. Chem.* **1989**, *54*, 1657.
[26] M. J. S. Dewar, E. G. Zoebisch, E. F. Healy, J. J. P. Stewart, *J. Am. Chem. Soc.* **1985**, *107*, 3902.
[27] W. L. Jorgensen, J. Tirado-Rives, *J. Am. Chem. Soc.* **1988**, *110*, 1657.

Received July 6, 1998